Molecular dynamics simulation of nickel-coated graphene bending

Konstantin P. Katin[1,2] ✉, *Vladimir S. Prudkovskiy*[2,3], *Mikhail M. Maslov*[1,2]

[1]*Department of Condensed Matter Physics, National Research Nuclear University 'MEPhI', Kashirskoe Shosse 31, Moscow 115409, Russia*
[2]*Laboratory of Computational Design of Nanostructures, Nanodevices and Nanotechnologies, Research Institute for the Development of Scientific and Educational Potential of Youth, Aviatorov Street 14/55, Moscow 119620, Russia*
[3]*Department of Physics, University of Crete, Heraklion 71003, Greece*
✉ *E-mail: KPKatin@yandex.ru*

Published in Micro & Nano Letters; Received on 20th June 2017; Revised on 8th August 2017; Accepted on 1st September 2017

The work presents a force field molecular dynamics study of nickel-coated graphene sheet bending at temperatures 300 and 1300 K. Nickel film is represented by nickel atoms located above the centres of carbon hexagons. Parameters for carbon–nickel interaction are fitted with regard to the accurate density functional calculations. Unstrained or flat configuration of the nickel–graphene system is found to be energetically unfavourable for the considered temperatures. Two types of curvatures are taken into account. Positive curvature is characterised by the nickel atoms located closer to the bending axis than the carbon ones, and negative curvature corresponds to the reverse atomic positions. It is found that the equilibrium radius for the curved nickel–graphene complex with the negative curvature is less than the corresponding value for the positive one. However, in both cases the equilibrium curvature radius of nickel-coated graphene is of the order of several nanometres. It is shown that both temperature and bending directions (zigzag and armchair) weakly affect the bending energy and do not change the equilibrium radius. Bending behaviour of the system is defined by the carbon–nickel interaction rather than the individual properties of isolated graphene and nickel films.

1. Introduction: A number of nickel–graphene structures are regarded as promising advanced materials. Nickel–graphene composites synthesised by electroplating in 2015 possess improved mechanical properties in comparison with the pure nickel [1]. Nickel passivation with the graphene grown by chemical vapor deposition (CVD) graphene allows one to use it as an oxidation-resistant electrode for spintronic devices [2]. Nickel-doped activated mesoporous carbon microspheres can serve as supercapacitors [3]. Nickel can be also used as a catalyst for graphene synthesis from polymers [4] and for transformation of graphene flakes to fullerenes [5].

The nickel-coated carbon nanotubes and graphene are of particular interest for various applications [6–8]. In such structures nickel is uniformly distributed on the carbon surface that leads to the significant modification of their properties. Moreover, nickel coating allows one to embed carbon structures into the aluminium [9] or gold [10] matrices. Nickel-coated nanotubes can be synthesised by electron-beam evaporation [11]. They possess the metallic behaviour regardless of their chirality. Nickel strongly affects the mechanical [12–14] and thermal [15] properties of the pristine nanotubes. Molecular dynamics (MD) studies of nickel-coated graphene also reveal the influence of nickel on the kinetic and mechanical properties of graphene sheet [16–18]. Galashev *et al.* [16, 18] show that the nickel films on graphene retain their stability even at very high temperatures up to 1800 K.

Recently, Hu *et al.* [19] proposed an efficient electroless Ni-plating method for the nickel–graphene sheets synthesis. In the obtained nickel–graphene composite, nickel atoms demonstrated high dispersion without aggregation. Stacking of nickel-coated sheets resulted in formation of pores with the average size ~4 nm [19]. This fact confirms that the nickel-coated sheets tend to become crumpled with the curvature radius of several nanometres instead of remain flat. However, in the previous calculations [16–18] the authors considered the absolutely flat sheet under periodical boundary conditions that is not suitable for crumpling modelling. At the same time, graphene on the rigid substrate not always remains flat [20–27]. In the latest years, the morphologies of graphene on the corrugated surface [20–23] and substrate-supported nanowires [24] or nanoparticles [25] were studied in detail. It was shown that the graphene curvature can be efficiently tuned through the substrate roughness [20–23]. Graphene can be flat or partial conformation to the substrate depending on its size [22] and thickness [20] as well as the geometries of the substrate corrugations [20–23, 26, 27] or nanoparticles [24, 25].

Here we present a MD study of nickel-coated graphene flake bending. We reveal the energetically favourable curvature for such systems at both room and high temperatures.

2. Computational details: In our study graphene is represented by square 4×4 nm^2 C_{678} carbon cluster, and 304 nickel atoms are placed above the centres of hexagons on the same side of the carbon monolayer. Such position of nickel atoms was used earlier in [12–14] to simulate the nickel-coated carbon nanotubes. In addition, recent theoretical studies in the frame of density functional theory confirm that such location of nickel atoms on the graphene surface is the most energetically favourable one [28].

To simulate the curved graphene, we transform flat carbon network to the part of cylinder surface with the radius R retaining all C–C distances unchanged. It should be noted that flat nickel-coated graphene was obtained by the method of structural relaxation so that the corresponding initial configuration relaxed to a state with an energy minimum under the influence of intramolecular forces only. The edge carbon atoms stay fixed under the relaxation (Fig. 1). The cylinder main axis can be perpendicular to the zigzag (see Fig. 1*a*) or to the armchair (see Fig. 1*b*) direction. During the MD simulations carbon atoms on the two cluster boundaries parallel to the cylinder main axis remain fixed to retain the constant curvature, as it is presented in Fig. 1. The curvature k of the surface is defined as $k = \pm 1/R$, where the 'minus' sign is used for the case when the nickel atoms are inside the carbon cylinder (i.e. they are closer to the cylinder axis than the carbon ones), and 'plus' sign corresponds to the case when the nickel atoms are outside the carbon cylinder.

For every MD run the corresponding initial curved configuration was constructed from the flat sample as it was described above. MD simulations are carried out using the velocity Verlet algorithm for

© The Institution of Engineering and Technology 2017

doi: 10.1049/mnl.2017.0460

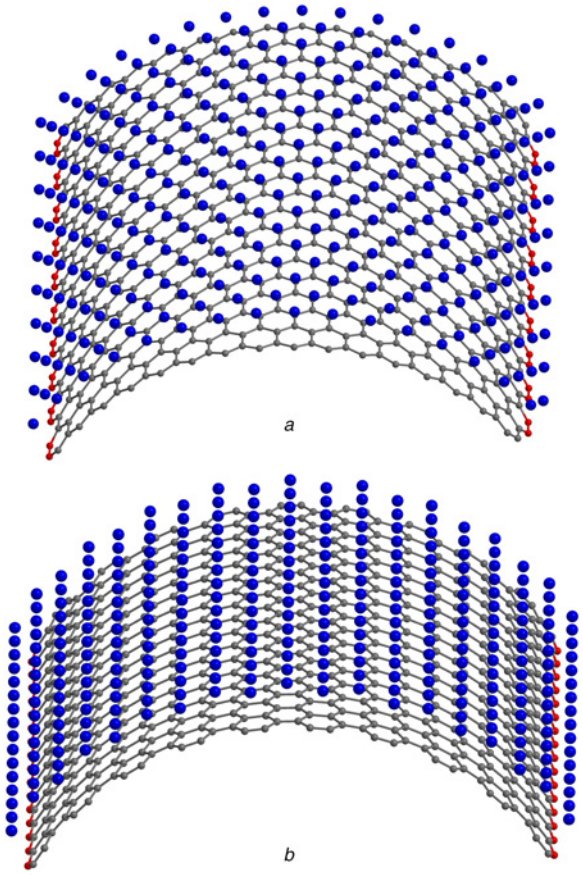

Fig. 1 *Atomistic model of nickel-coated graphene cluster $C_{678}Ni_{304}$ with*
a Zigzag curvature
b Armchair curvature
Blue, grey, and red spheres correspond to nickel, free, and fixed carbon atoms, respectively

the total period of time 2 ns with the time step 0.2 fs. In order to provide the constant temperature, we replace the velocities of all atoms in the system by the Maxwell distributed random values every 50 fs. Such procedure is rather effective for the simulation of the system interaction with the thermostat [29, 30]. Thermalisation of the system occurs during the first nanosecond, then the potential energy of the system is calculated every 10 fs and averaged. MD calculations were carried out for room temperature (300 K) and for $T = 1300$ K. Note that for the MD simulations our own Fortran program based on the empirical potential presented below was used.

The potential energy U of the carbon–nickel system is defined as a sum of three terms

$$U = U^{\mathrm{C-C}} + U^{\mathrm{Ni-Ni}} + U^{\mathrm{C-Ni}}, \tag{1}$$

that describe carbon–carbon, nickel–nickel, and carbon–nickel interactions, respectively.

The first term $U^{\mathrm{C-C}}$ is calculated as a sum of the Brenner many-body empirical potential [31] and the Lennard-Jones pair non-covalent attraction with the parameters adopted from [32]. The second term $U^{\mathrm{Ni-Ni}}$ is obtained using the bond-order approach proposed by Shibuta and Maruyama [33]. The last term $U^{\mathrm{C-Ni}}$ can be calculated in the frame of the same approach [33] as it was done in [12, 34]. However, parameters of this model are derived from the density functional calculations of small clusters NiC, NiC_3, and NiC_4, that are significantly different from the nickel–graphene system considered in this work. Thus, the transferability of this model raises some doubts. A number of recent studies used the sum of pair Morse terms for the description of carbon–nickel interaction [16, 17, 35–37]

$$U^{\mathrm{C-Ni}} = \sum U_0 \left[\left(1 - \mathrm{e}^{-\beta\left(r^{\mathrm{C-Ni}} - R_e\right)} \right)^2 - 1 \right], \tag{2}$$

where the summation is performed for all carbon–nickel atomic pairs, $r^{\mathrm{C-Ni}}$ is the distance between the carbon and the nickel atom, U_0, β, and R_e are the fitting parameters. It was shown that the different values of these parameters led to the qualitatively different interaction character between the nickel nanoparticle and the carbon nanotube [29]. Therefore, the correct choice of the parameter set is one of the crucial problems.

To describe adequately the C–Ni interaction in curved nickel-coated graphene, we choose C_{240} fullerene with adsorbed Ni atom on its surface as a relevant system for approbation the different C–Ni interaction models. We find the equilibrium position of nickel atom above the centre of carbon hexagon, and calculate the adsorption energy E_a, mean C–Ni distance $l_{\mathrm{C-Ni}}$, and second derivative of total energy with respect to coordinate $\partial^2 U/\partial r^2$ using different methods. Adsorption energy is defined as

$$E_a = U\left(\mathrm{C_{240}Ni}\right) - U\left(\mathrm{C_{240}}\right) - U(\mathrm{Ni}), \tag{3}$$

where $U(\mathrm{C_{240}Ni})$, $U(\mathrm{C_{240}})$, and $U(\mathrm{Ni})$ are the total energies of fullerene-nickel complex, fullerene C_{240}, and isolated nickel atom, respectively. Geometry optimisation is performed using the Newton–Raphson method until the residual forces acting on atoms are <0.005 eV/Å. The value of $l_{\mathrm{C-Ni}}$ is defined as the arithmetic mean of the six distances between the nickel atom and the vertices of corresponding carbon hexagon (these six distances may vary slightly from the average for ~0.1 Å [38]). The second derivative of total energy with respect to coordinate is defined as

$$\frac{\partial^2 U}{\partial r^2} = \frac{U(r_0 + \Delta r) + U(r_0 - \Delta r) - 2U(r_0)}{\Delta r^2}, \tag{4}$$

where $U(r_0 + \Delta r)$, $U(r_0 - \Delta r)$, and $U(r_0)$ are the total energies of $C_{240}Ni$ complexes where Ni atom is located at distances of $r_0 + \Delta r$, $r_0 - \Delta r$, and r_0 from the hexagon plane, respectively. Note that r_0 is the equilibrium distance specified by the method of calculation, and Δr is equal to 0.05 Å for all considered methods.

Results obtained using various empirical approaches are further compared with the more accurate data computed by means of density functional theory using the TeraChem program package [39–42]. Restricted open-shell formalism is applied. The Perdew–Burke–Ernzerhof functional with the 6-311G(d,p)/LANL2DZ multibasis set is used [43–47]. Grimme's D3 dispersion corrections [48] are also taken into account. All obtained data are summarised in Table 1.

As one can see from Table 1, the bond order potential [33] as well as two parameter sets for Morse potential used in [35, 36] cannot describe the interaction between the nickel atom and fullerene surface correctly. Therefore, we present original Morse parameters that reproduce exactly the DFT-D3 data for the $C_{240}Ni$ complex (they are also presented in Table 1). In our opinion, these parameters are more suitable for curved nickel-coated graphene simulation especially when the nickel atoms are located near their equilibrium positions above the centres of carbon hexagons. Thus, we use them in the present study.

3. Results and discussion: We obtain the dependence of mean potential energy ΔU of bent $C_{678}Ni_{304}$ cluster on its zigzag and armchair curvatures k. Calculation results are presented in Fig. 2. Note that the energy of unstrained (i.e. flat) cluster is taken as a reference point. The general appearance of such dependence is

© The Institution of Engineering and Technology 2017

Table 1 Adsorption energies E_a, mean C–Ni distances $l_{C–Ni}$, and second derivatives of the total energy $\partial^2U/\partial r^2$ calculated for the $C_{240}Ni$ complex using different theoretical approaches. Corresponding Morse parameters are also presented (see (2))

Method	Morse parameters			Calculated data		
	U_0, eV	B, 1/Å	R_e, Å	E_a, eV	$l_{C–Ni}$, Å	$\partial^2U/\partial r^2$, eV/Å^2
bond order [33]	—	—	—	7.46	1.990	12.15
Morse I [35]	2.431	3.295	1.763	18.17	1.726	42.04
Morse II [36]	0.3	2.0	2.0	4.02	1.719	2.05
Morse III (this work)	0.433	3.244	2.316	4.28	2.191	9.14
DFT-D3	—	—	—	4.28	2.191	9.14

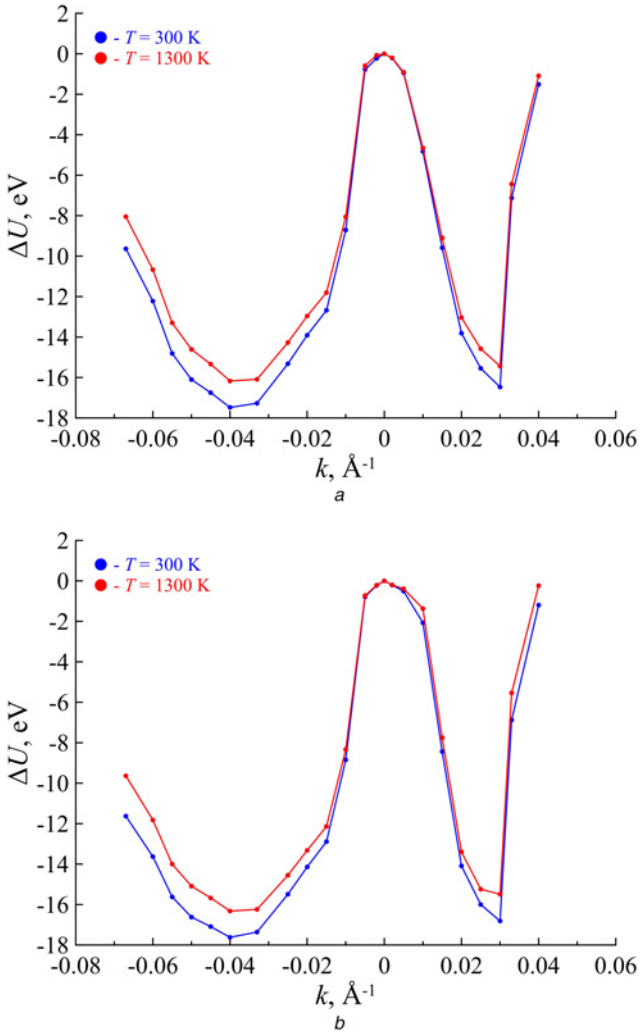

Fig. 2 *Mean potential energy ΔU of curved $C_{678}Ni_{304}$ cluster as a function of*
a Zigzag curvature
b Armchair curvature *k* at $T = 300$ K (blue) and $T = 1300$ K (red)
Energy of unstrained (i.e. flat) cluster is taken as a reference point

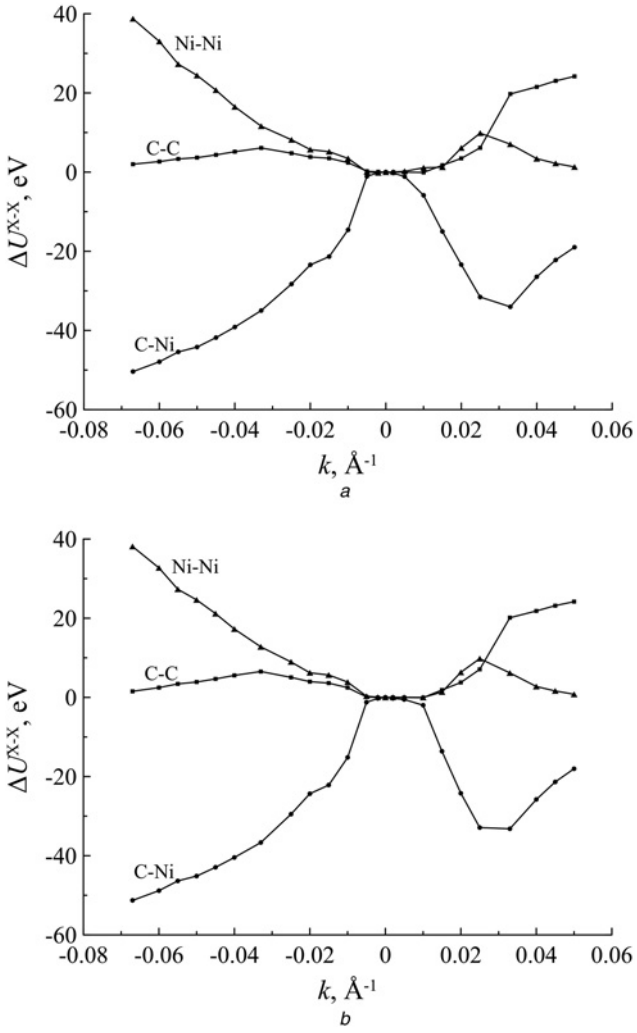

Fig. 3 *Mean potential energy components $\Delta U^{X–X}$ ($X = C$, Ni) of curved $C_{678}Ni_{304}$ cluster as a function of*
a Zigzag curvature
b Armchair curvature *k* at $T = 300$ K
Energy components of unstrained (i.e. flat) cluster are taken as reference points

the same for both zigzag and armchair curvature directions and for different temperatures 300 and 1300 K. Unstrained (flat) configuration of the $C_{678}Ni_{304}$ cluster is found to be energetically unfavourable. Maximum energy gains are achieved at negative curvature (nickel inside) corresponding to the radius $R = 25$ Å. They are equal to 26 and 24 meV per carbon atom at $T = 300$ and $T = 1300$ K, respectively. For the positive curvature (nickel outside) maximum energy gains are achieved at $R = 35$ Å. They are equal to 24 and 23 meV per carbon atom at $T = 300$ and $T = 1300$ K, respectively. These values are of the same order of magnitude as the typical van-der-Waals interaction of graphene with the substrate. Therefore, the presence of substrate under graphene can prevent the bending.

Note that the global energy minima correspond to the configuration with the negative curvature. This fact is rather unexpected due to the lattice constants mismatch of graphene and nickel film. The distance between the centres of neighbouring hexagons in ideal graphene is equal to $1.42\sqrt{3} \approx 2.46$ Å. According to the model [33], the optimal distance between the six-coordinated

© The Institution of Engineering and Technology 2017

doi: 10.1049/mnl.2017.0460

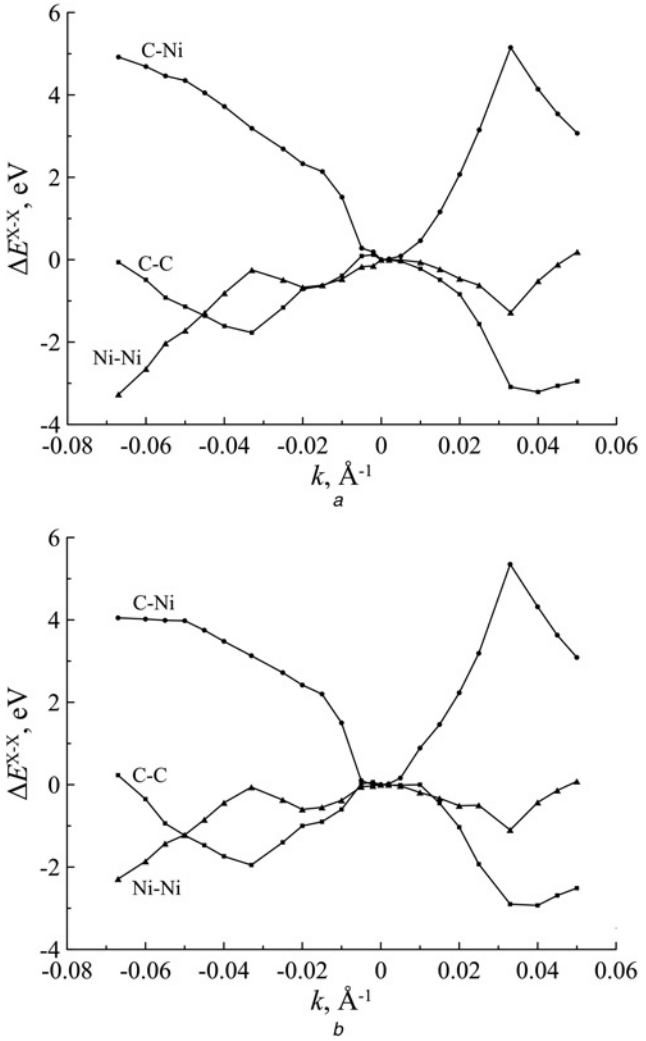

Fig. 4 *Differences $\Delta E^{X–X}$ (X = C, Ni) of mean potential energy components $\Delta U^{X–X}$ at T = 1300 K and T = 300 K for curved $C_{678}Ni_{304}$ cluster as a function of*
a Zigzag curvature
b Armchair curvature k
Energy components $\Delta U^{X–X}$ of unstrained (i.e. flat) cluster are taken as reference points

nickel atoms is slightly higher (~1%). It is expected that nickel–graphene system will tend to the geometry with the positive curvature to release the strain. However, the configuration with negative curvature is more favourable. Thus, the stretching/compressing of nickel and carbon sheets plays a minor role in the bending of graphene–nickel system considered.

To provide the further insight we regard the dependence of every component of mean potential energy $\Delta U^{C–C} = U^{C–C}(k) – U^{C–C}(0)$, $\Delta U^{Ni–Ni} = U^{Ni–Ni}(k) – U^{Ni–Ni}(0)$, and $\Delta U^{C–Ni} = U^{C–Ni}(k) – U^{C–Ni}(0)$ on k. The energies $U^{C–C}(0)$, $U^{Ni–Ni}(0)$, and $U^{C–Ni}(0)$ correspond to the energies of the unstrained system with zero curvature. They are taken as the reference points. Results obtained for the case of zigzag (Fig. 3*a*) and armchair (Fig. 3*b*) bending directions differ from each other very slightly. One can see that both $\Delta U^{C–C}$ and $\Delta U^{Ni–Ni}$ are positive at any non-zero k due to the contribution of the graphene and nickel film elastic deformation energies arising from bending.

Only $\Delta U^{C–Ni}$ component is negative, but it has the highest absolute value at any non-zero $k < 0.03$ 1/Å. This component defines the system tendency to become curved rather than flat. At high positive curvatures ($k > 0.03$ 1/Å) the graphene–nickel interaction becomes weaker. Thus, the nickel film partially relaxes and reduces its energy. From Fig. 2 one can see that the temperature increase from 300 to 1300 K does not change the optimal curvatures and slightly (~1 meV per carbon atom) decreases the energy difference between the curved and flat configurations. Fig. 4 presents the energy differences $\Delta E^{C–C} = \Delta U^{C–C}(1300\text{ K}) – \Delta U^{C–C}(300\text{ K})$, $\Delta E^{Ni–Ni} = \Delta U^{Ni–Ni}(1300\text{ K}) – \Delta U^{Ni–Ni}(300\text{ K})$, and $\Delta E^{C–Ni} = \Delta U^{C–Ni}(1300\text{ K}) – \Delta U^{C–Ni}(300\text{ K})$ as a function of zigzag and armchair curvatures (Figs. 4*a* and *b*, respectively). High temperatures facilitate the bending of both graphene and nickel films regarded separately. At the same time, more intensive contribution of carbon–nickel interaction leads to the opposite result. Finally, high temperatures tend to make the bending process less favourable, but this effect in insignificant in the range of T = 300–1300 K.

4. Conclusion: In this Letter, the bending of nickel-coated graphene flake was studied. We found that the bending of such system leads to the energy gain ~25 meV per carbon atom. Equilibrium curvatures correspond to a few nanometres radii and depend on the curvature sign of the system. Bending direction (zigzag or armchair) has the minor impact on the process. Temperature rise tends to hinder the bending effect, but remains negligible up to 1300 K.

The bending mechanism of nickel-coated graphene is not determined by a simple sum of such characteristics of graphene and nickel films. It is dominated by carbon–nickel interaction in this complex and qualitatively differs from the bending behaviour of carbon and nickel components regarded separately. Note that the empirical transferable potential obtained for this study can be successfully generalised to the other carbon–nickel systems, such as doped fullerenes, nickel-coated phagraphene or carbon nanotubes, nickel clusters on the wrinkled and crumpled graphenes [49, 50]. In addition, the results presented here confirm the tendency of the nickel-coated graphene to become crumpled rather than flat that qualitatively explains the appearance of nanometre sized pores in nickel–graphene composites prepared recently [19].

5. Acknowledgments: The reported study was funded by Russian Foundation for Basic Research (RFBR), according to the research project no. 16 32-60081 mol_a_dk.

6 References

[1] Ren Z., Meng N., Shehzad K., *ET AL.*: 'Mechanical properties of nickel–graphene composites synthesized by electrochemical deposition', *Nanotechnology*, 2015, **26**, (6), p. 065706
[2] Dlubak B., Martin M.-B., Weatherup R.S., *ET AL.*: 'Graphene-passivated nickel as an oxidation-resistant electrode for spintronics', *ACS Nano*, 2012, **6**, (12), pp. 10930–10934
[3] Liu M., Gan L., Xiong W., *ET AL.*: 'Nickel-doped activated mesoporous carbon microspheres with partially graphitic structure for supercapacitors', *Energy Fuels*, 2013, **27**, (2), pp. 1168–1173
[4] Kwon H., Ha J.M., Yoo S.H., *ET AL.*: 'Synthesis of flake-like graphene from nickel-coated polyacrylonitrile polymer', *Nanoscale Res. Lett.*, 2014, **9**, p. 618
[5] Lebedeva I.V., Knizhnik A.A., Popov A.M., *ET AL.*: 'Ni-assisted transformation of graphene flakes to fullerenes', *J. Phys. Chem. C*, 2012, **116**, (11), pp. 6572–6584
[6] Seenithurai S., Pandyan R.K., Kumar S.V., *ET AL.*: 'H_2 adsorption in Ni and passivated Ni doped 4 Å single walled carbon nanotube', *Int. J. Hydrogen Energy*, 2013, **38**, (18), pp. 7376–7381
[7] Ihsanullah A.A., Al-Amer A.M., Laoui T., *ET AL.*: 'Heavy metal removal from aqueous solution by advanced carbon nanotubes: critical review of adsorption applications', *Separation Purif. Technol.*, 2015, **157**, pp. 141–161
[8] Hooijdonk E.V., Bittencourt C., Snyders R., *ET AL.*: 'Functionalization of vertically aligned carbon nanotubes', *Beilstein J. Nanotechnol.*, 2013, **4**, pp. 129–152
[9] Song H.-Y., Zha X.-W.: 'Influence of nickel coating on the interfacial bonding characteristics of carbon nanotube-aluminum composites', *Comput. Mat. Sci.*, 2010, **49**, (4), pp. 899–903

© The Institution of Engineering and Technology 2017

[10] Song H.-Y., Zha X.-W.: 'Mechanical properties of nickel-coated single-walled carbon nanotubes and their embedded gold matrix composites', *Phys. Lett. A*, 2010, **374**, (8), pp. 1068–1072
[11] Zhang Y., Franklin N.W., Chen R.J., *ET AL.*: 'Metal coating on suspended carbon nanotubes and its implication to metal-tube interaction', *Chem. Phys. Lett.*, 2000, **331**, (1), pp. 35–41
[12] Inoue S., Matsumura Y.: 'Influence of metal coating on single-walled carbon nanotube: molecular dynamics approach to determine tensile strength', *Chem. Phys. Lett.*, 2009, **469**, pp. 125–129
[13] Song H.-Y., Zha X.-W.: 'Molecular dynamics study of effects of nickel coating on torsional behavior of single-walled carbon nanotube', *Phys. B, Cond. Matt.*, 2011, **406**, (4), pp. 992–995
[14] Zhu F., Liao H., Tang K., *ET AL.*: 'Molecular dynamics study on the effect of temperature on the tensile properties of single-walled carbon nanotubes with a Ni-coating', *J. Nanomater.*, 2015, **2015**, p. 767182
[15] Inoue S., Matsumura Y.: 'Metal coating effect on thermal diffusivity of single-walled carbon nanotube', *Chem. Phys. Lett.*, 2010, **495**, pp. 80–83
[16] Galashev A.E., Polukhin V.A.: 'Computer simulation of thin nickel films on single-layer graphene', *Phys. Solid State*, 2013, **55**, (11), pp. 2368–2373
[17] Galashev A.E.: 'Computer simulation of heating of nickel films on two-layer graphene', *Phys. Solid State*, 2014, **56**, (5), pp. 1048–1053
[18] Galashev A.E.: 'Computer simulation of the thermal stability of nickel films on two-layer graphene', *High Temp.*, 2014, **52**, (5), pp. 633–639
[19] Hu Q.-H., Wang X.-T., Chen H., *ET AL.*: 'Synthesis of Ni/graphene sheets by an electroless Ni-plating method', *New Carbon Mater.*, 2012, **27**, (1), pp. 35–41
[20] Gao W., Huang R.: 'Effect of surface roughness on adhesion of graphene membranes', *J. Phys. D, Appl. Phys.*, 2011, **44**, p. 452001
[21] Li T., Zhang Z.: 'Substrate-regulated morphology of graphene', *J. Phys. D, Appl. Phys.*, 2010, **43**, p. 075303
[22] Chen H., Yao Y., Chen S.: 'Adhesive contact between a graphene sheet and a nano-scale corrugated surface', *J. Phys. D, Appl. Phys.*, 2013, **46**, p. 205303
[23] Zhang Z., Li T.: 'Determining graphene adhesion via substrate-regulated morphology of graphene', *J. Appl. Phys.*, 2011, **110**, p. 083526
[24] Zhang Z., Li T.: 'Graphene morphology regulated by nanowires patterned in parallel on a substrate surface', *J. Appl. Phys.*, 2010, **107**, p. 103519
[25] Zhu Z., Li T.: 'Wrinkling instability of graphene on substrate-supported nanoparticles', *J. Appl. Mech.*, 2014, **81**, p. 061008
[26] Zhou Y., Chen Y., Liu B., *ET AL.*: 'Mechanics of nanoscale wrinkling of graphene on a non-developable surface', *Carbon*, 2015, **84**, pp. 263–271
[27] Chen Y., Ma Y., Wang S., *ET AL.*: 'The morphology of graphene on a non-developable concave substrate', *Appl. Phys. Lett.*, 2016, **108**, p. 031905
[28] Mashhadzadeh A.H., Vahedi A.M., Ardjmand M., *ET AL.*: 'Investigation of heavy metal atoms adsorption onto graphene and graphdiyne surface: a density functional theory study', *Superlattices Microstruct.*, 2016, **100**, pp. 1094–1102
[29] Attard P.: 'Stochastic molecular dynamics: a combined Monte Carlo and molecular dynamics technique for isothermal simulations', *J. Chem. Phys.*, 2002, **116**, p. 9616
[30] Podlivaev A.I., Katin K.P.: 'On the dependence of the lifetime of an atomic cluster on the intensity of its heat exchange with the environment', *JETP Lett.*, 2010, **92**, (1), pp. 52–56
[31] Brenner D.W.: 'Empirical potential for hydrocarbons for use in simulating the chemical vapor deposition of diamond films', *Phys. Rev. B*, 1990, **42**, pp. 9458
[32] Stuart S.J., Tutein A.B., Harrison J.A.: 'A reactive potential for hydrocarbons with intermolecular interactions', *J. Chem. Phys.*, 2000, **112**, p. 6472
[33] Shibuta Y., Maruyama S.: 'Bond-order potential for transition metal carbide cluster for the growth simulation of a single-walled carbon nanotube', *Comput. Mat. Sci.*, 2007, **39**, (4), pp. 842–848
[34] Neyts E.C., Bogaerts A.: 'Formation of endohedral Ni@C_{60} and exohedral Ni-C_{60} metallofullerene complexes by simulated ion implantation', *Carbon*, 2009, **47**, (4), pp. 1028–1033
[35] Lyalin A., Hussien A., Solov'yov A.V., *ET AL.*: 'Impurity effect on the melting of nickel clusters as seen via molecular dynamics simulations', *Phys. Rev. B*, 2009, **79**, p. 165403
[36] Moseler M., Cervantes-Sodi F., Hofmann S., *ET AL.*: 'Dynamic catalyst restructuring during carbon nanotube growth', *ACS Nano*, 2010, **4**, (12), pp. 7587–7595
[37] Verkhovtsev A.V., Schramm S., Solov'yov A.V.: 'Molecular dynamics study of the stability of a carbon nanotube atop a catalytic nanoparticle', *Eur. Phys. J. D*, 2014, **68**, p. 246
[38] Yagi Y., Briere T.M., Sluiter M.H.F., *ET AL.*: 'Stable geometries and magnetic properties of single-walled carbon nanotubes doped with 3*d* transition metals: a first-principles study', *Phys. Rev. B*, 2004, **69**, p. 075414
[39] Ufimtsev I.S., Martínez T.J.: 'Quantum chemistry on graphical processing units. 3. analytical energy gradients, geometry optimization, and first principles molecular dynamics', *J. Chem. Theory Comput.*, 2009, **5**, (10), pp. 2619–2628
[40] Titov A.V., Ufimtsev I.S., Luehr N., *ET AL.*: 'Generating efficient quantum chemistry codes for novel architectures', *J. Chem. Theory Comput.*, 2013, **9**, (1), pp. 213–221
[41] Kästner J., Carr J.M., Keal T.W., *ET AL.*: 'DL-FIND: an open-source geometry optimizer for atomistic simulations', *J. Phys. Chem. A*, 2009, **113**, (43), pp. 11856–11865
[42] Goumans T.P.M., Catlow C.R.A., Brown W.A., *ET AL.*: 'An embedded cluster study of the formation of water on interstellar dust grains', *Phys. Chem. Chem. Phys.*, 2009, **11**, pp. 5431–5436
[43] Perdew J.P., Burke K., Ernzerhof M.: 'Generalized gradient approximation made simple', *Phys. Rev. Lett.*, 1996, **77**, p. 3865
[44] Krishnan R., Binkley J.S., Seeger R., *ET AL.*: 'Self-consistent molecular orbital methods. XX. A basis set for correlated wave functions', *J. Chem. Phys.*, 1980, **72**, p. 650
[45] Wadt W.R., Hay P.J.: '*Ab initio* effective core potentials for molecular calculations. Potentials for the transition metal atoms Sc to Hg', *J. Chem. Phys.*, 1985, **82**, p. 270
[46] Wadt W.R., Hay P.J.: '*Ab initio* effective core potentials for molecular calculations. Potentials for main group elements Na to Bi', *J. Chem. Phys.*, 1985, **82**, p. 284
[47] Wadt W.R., Hay P.J.: '*Ab initio* effective core potentials for molecular calculations. Potentials for K to Au including the outermost core orbitals', *J. Chem. Phys.*, 1985, **82**, p. 299
[48] Grimme S., Antony J., Ehrlich S., *ET AL.*: 'A consistent and accurate ab initio parametrization of density functional dispersion correction (DFT-D) for the 94 elements H-Pu', *J. Chem. Phys.*, 2010, **132**, p. 154104
[49] Deng S., Berry V.: 'Wrinkled, rippled and crumpled graphene: an overview of formation mechanism, electronic properties, and applications', *Mater. Today*, 2016, **19**, pp. 197–212
[50] ElRouby W.M.A.: 'Crumpled graphene: preparation and applications', *RSC Adv.*, 2015, **5**, pp. 66767–66796

© The Institution of Engineering and Technology 2017

doi: 10.1049/mnl.2017.0460